Available online at www.sciencedirect.com
ScienceDirect
Ceramics International 36 (2010) 69–73
CERAMICS INTERNATIONAL
www.elsevier.com/locate/ceramint

# Effect of temperature on lateral growth of ZnO grains grown by MOCVD

Y.J. Chen [a,b], Y.Y. Shih [a,b], C.H. Ho [a,b], J.H. Du [a,b], Y.P. Fu [a,b,*]

[a] *Department of Materials Science and Engineering, National Donghwa University, Shoufeng, Hualien 97401, Taiwan*
[b] *Graduate Institute of Optoelectronics Engineering, Shoufeng, Hualien 97401, Taiwan*

Received 21 April 2009; received in revised form 29 May 2009; accepted 30 June 2009
Available online 17 July 2009

## Abstract

ZnO growth on sapphire by MOCVD using dimethylzinc and $CO_2$ as zinc and oxygen precursors was performed. A dense ZnO film with major (0 0 0 2) orientation can be prepared at 350 °C and above with high dimethylzinc flow rate. Result shows that the growth temperature suppresses the lateral growth of ZnO grains, promotes the coalescence of grains but reduces the crystal alignment. To further enhance the crystal alignment, a two-step temperature variation growth method is proposed. Using the two-step growth method, employing the initial growth at lower temperature followed by the growth at higher temperature, a densely packed ZnO film with larger grains and well-aligned (0 0 0 2) crystallographic orientation can be obtained. The effect of temperature on nucleation and growth rate, and its relation to the crystal alignment enhancement is also discussed.

*Keywords:* A. Films; A. Grain growth; D. ZnO; Metal-organic chemical vapor deposition

## 1. Introduction

ZnO is an attractive material potential for applications such as light-emitting diodes [1,2], photodetectors [3,4], varistors [5], gas sensors [6,7], surface acoustic wave filters [8], transparent conducting oxide [9–11], and optical modulator waveguides [12]. Among these applications, the blue optoelectronic application receives much attention because ZnO has unique properties that fulfill the requirement. With direct bandgap of 3.3 eV and a high exciton binding energy of 60 meV, ZnO is a potential candidate for blue optoelectronics [13–16], and is even considered competitor for the well recognized GaN in the field of blue LEDs and LDs [17]. However, the growth of the ZnO film for such applications still remains a problem [18]. Thin film of epitaxial quality is often required, but the crystallographic anisotropy of the ZnO's wurtzite structure limits the achievement of the goal. The growth rate anisotropy of the hexagonal symmetry results in the formation of hexagonal nanorods and nanowires [19–22], and producing a porous ZnO film. How to prepare dense film without the formation of nanorod structure is urgent to realize ZnO's practical usage.

It is known that the low VI/II ratio promotes the lateral growth of the ZnO grains [23]. To enhance the lateral growth in hope that all nanorods are in close contact and become densely packed, $CO_2$ is chosen in place of $O_2$ as the oxygen source in this study for the growth. The $CO_2$ provides much lower oxygen partial pressure than $O_2$ in the MOCVD process [24], so it provides much lower VI/II ratio environment.

In this study, we would like to explore the effect of temperature on ZnO growth by MOCVD. When VI/II ratio is largely reduced using $CO_2$ in place of $O_2$, the temperature may have significant effect on film morphology. Thus for the development of dense and large area thin film growth, we focus on the study of the temperature effect on ZnO film growth with low VI/II ratio. Furthermore, we would like to study if there is a way to further enhance the crystal alignment by growth temperature maneuver. We would like to demonstrate the crystal alignment enhancement of the film by a two-step temperature variation growth method. It is known that the nucleation and coalescence of grains is sensitive to the growth temperature. Using a two-step temperature variation growth model, the effect of the temperature variation on the nucleation and coalescence, and hence the subsequent effect on crystal alignment, can be explained satisfactorily.

---

* Corresponding author at: Department of Materials Science and Engineering, National Donghwa University, Shoufeng, Hualien 97401, Taiwan.
Tel.: +886 3 863 4227.
*E-mail address:* ypfu@mail.ndhu.edu.tw (Y.P. Fu).

0272-8842/$36.00 © 2009 Elsevier Ltd and Techna Group S.r.l. All rights reserved.
doi:10.1016/j.ceramint.2009.06.018

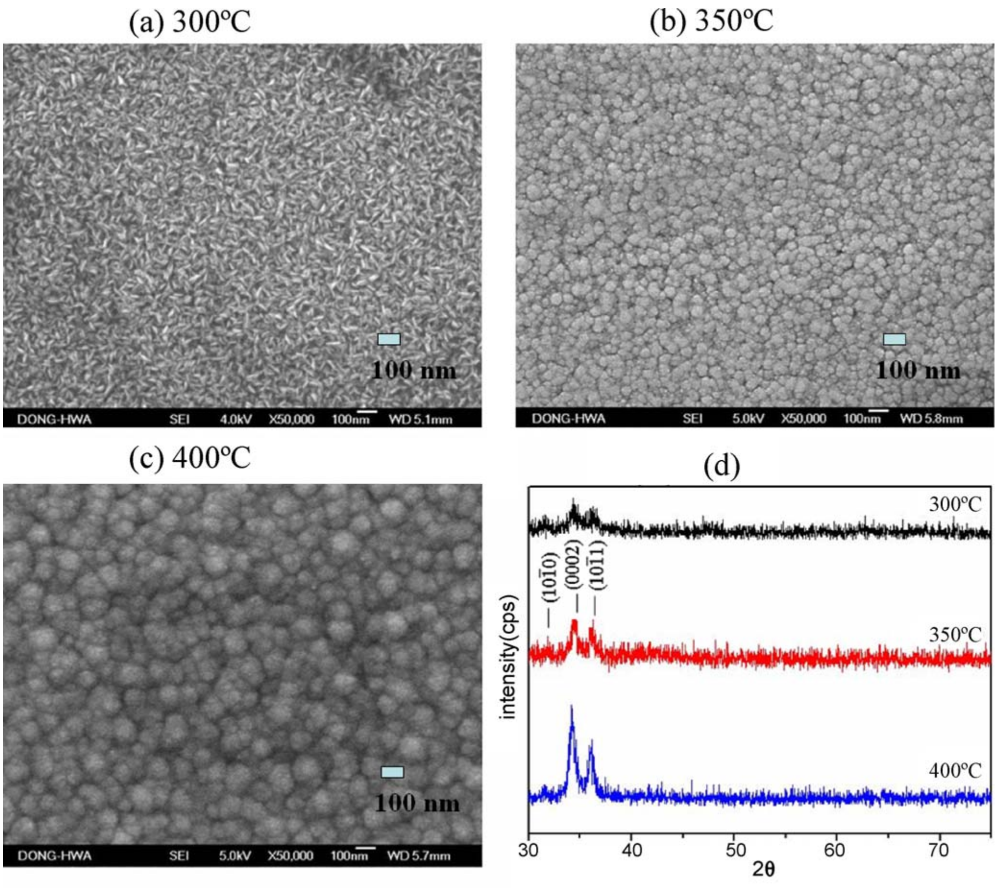

Fig. 1. The surface morphology of ZnO films (top view) grown using high flow rates of DMZn (0.58 sccm) and grown at (a) 300 °C, (b) 350 °C, (c) 400 °C, and (d) their respective XRD spectra.

## 2. Experimental procedure

The experiment was performed using $CO_2$ as the oxygen precursor. Dimethylzinc (DMZn) was used as zinc precursor. The $CO_2$ flow rate was 1000 sccm while the dimethylzinc flow rate was 0.58 sccm. The precursors were mixed together and flow into the deposition chamber through a showerhead nozzle with showerhead diameter of 100 mm. The substrate was placed right beneath the showerhead. The chamber pressure was kept at 200 Torr with the help of balanced argon flow. The growth experiment was performed at three different substrate temperatures of 300 °C, 350 °C, and 400 °C. The substrate was c-plane sapphire, and the growth time was 20 min. The temperature variation experiment is also made for the growth with temperature rises linearly from 350 °C to 400 °C for the first 5 min, and maintained at 400 °C for the remaining 15 min. Field emission SEM, JEOL JSM-6500F, were used to observe the microstructure of the deposit, and the $\theta$–$2\theta$ scan of CuK$\alpha$ X-ray diffraction by Rigaku D/MAX-2500 V (40 kV, 100 mA) was used to determine the plane and crystallographic alignment of the ZnO film. Electrical conductivity was measured by two-point technique using Keithley 6485.

## 3. Results and discussion

The resultant film morphologies and corresponding X-ray diffraction patterns for the films grown at three different growth temperatures are shown in Fig. 1. In X-ray diffraction (XRD) patterns, (1 0 $\bar{1}$ 1) peak in addition to (0 0 0 2) were present [Fig. 1(d)]. Our previous study (not shown) [25] of ZnO growth using low DMZn flow rate of 0.09 sccm under the same $CO_2$ environment shows only (0 0 0 2) peak in the XRD patterns. The presence of (1 0 $\bar{1}$ 1) peak of this experiment suggests that some ZnO crystals lies somewhere off the perpendicular position. Note that the presence of (1 0 $\bar{1}$ 1) peak is for all three samples grown at different temperatures, indicating it is the increased DMZn and not necessarily the growth temperature that causes the presence of (10$\bar{1}$1) peaks. The more or less randomly distributed ZnO orientation can be resorted to the high deposition rate caused by the increase of DMZn flow rate. The nucleation and growth rate increase by high deposition rate is a common phenomenon and is well documented [26]. Since the high deposition rate results in high nucleation rate and high growth rate of ZnO, the Zn and O atoms does not have enough time to diffuse to their optimum sites on substrate, resulting more or less randomly oriented ZnO crystals.

The growth at 300 °C shows a special ‘‘grassy’’ morphology shown in Fig. 1(a). The XRD pattern for sample grown at 300 °C does not have strong (0 0 0 2) diffraction peak indicating most ZnO crystals do not have their [0 0 0 2] axis strictly perpendicularly aligned with respect to the substrate. Furthermore, the presence of (1 0 $\bar{1}$ 0) peak suggests that significant amount of crystals have their [0 0 0 2] axis parallel to the substrate. The

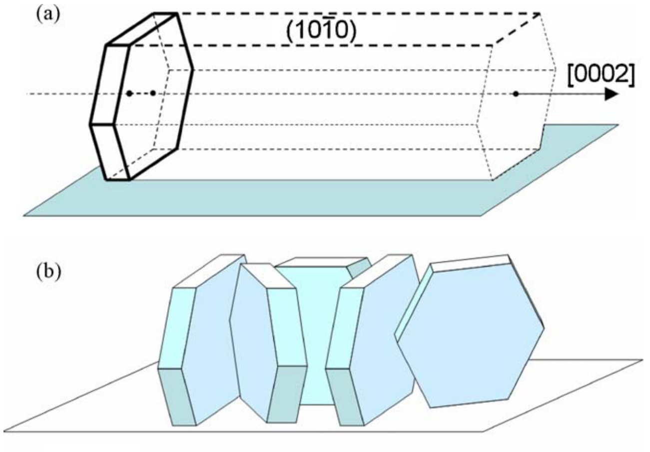

Fig. 2. The plane and direction of ZnO crystal when [0 0 0 2] axis is parallel to the substrate plane. (a) The formation of hexagonal disk from the hexagonal rod. (b) The schematic representation of the standing flakes for the grassy microstructure.

orientation of the ZnO crystal with $(1\,0\,\bar{1}\,0)$ reflection is illustrated in Fig. 2. The presence of $(1\,0\,\bar{1}\,0)$ in XRD pattern indicates that the $(1\,0\,\bar{1}\,0)$ plane of some crystals is parallel to the substrate plane since the $\theta$–$2\theta$ method of XRD can only reveal peaks from the crystallographic planes parallel to the substrate plane. As $(1\,0\,\bar{1}\,0)$ is parallel to the substrate plane, the [0 0 0 2] axis of the ZnO crystal should lie along the substrate plane. It is well known that the grains with highest growth direction perpendicular to the substrate will dominate the orientation of the film [27,28]. The presence of the ZnO crystals with axial direction lie along the substrate plane in the film suggests that the growth rate along the direction perpendicular to the axial direction of the ZnO crystals may exceed their growth rate along axial direction. When lateral growth rate exceeds axial growth rate of a hexagonal crystal, the shape of the crystal changes from hexagonal rod to hexagonal disk [Fig. 2(b)]. The grassy microstructure of the ZnO film [Fig. 1(a)] is thus determined as of hexagonal-shaped disks standing on the substrate plane. The significance of this finding of standing flakes is that the reduced temperature promotes the lateral growth over the axial growth of the ZnO rods.

Although lateral growth is enhanced at 300 °C, the film is still porous and the crystallographic orientation of ZnO is different from (0 0 0 2) growth. The growth at 350 °C has its morphology return to its normal (0 0 0 2) growth feature as can be seen from the equiaxial grains instead of ‘‘grassy’’ microstructure viewing from the top [Fig. 1(b)]. This finding suggests that the lateral growth of ZnO crystal is suppressed as temperature is raised to 350 °C, so that axial growth is higher than the radial growth rate of the crystal, and most of the crystals are grown with their axial direction perpendicular to the substrate. It also shows that even though lateral growth is suppressed by increased temperature, the increased DMZn flow rate enhanced the lateral growth so that the film is no longer composed of distinct nanorods. The film grown at 350 °C is more densely packed compared with that grown at 300 °C, attributed to the formation of major (0 0 0 2) grains and increased DMZn flow rate.

The growth at 400 °C shows also (0 0 0 2) growth. It also shows features of increased grain size at around 100 nm [Fig. 1(c)]. Two possible reasons may contribute to the increased grain size. One is the enhanced lateral growth of individual grains at 400 °C, the other is the grain coalescence that takes effect at elevated temperature. From the observation that the lateral growth is suppressed as temperature increases from 300 °C to 350 °C, the lateral growth of individual grains should be enhanced with reducing temperature and not with increasing temperature, so the lateral growth enhancement at 400 °C is unlikely. Thus we conclude that the grain size increase at 400 °C is largely due to coalescence. The increase of peak intensities in XRD pattern with temperature agrees with the fact that the coalescence of grains eliminates significant amount of grain boundaries and improves the crystal quality. The electrical conductivities of ZnO films grown at 350 °C, 400 °C, and with two-step growth are 0.375, 0.086, and $0.061\ \mathrm{S\ cm^{-1}}$, respectively. It is believed that the grain boundary provides the major conduction path for the carrier transport in the ZnO film, so that the film with larger grain size has less grain boundary area, and less conductivity, i.e. the larger the grain the lower the conductivity of the film. It matches the trend of the grain size variation observed by FESEM.

The films grown at 350 °C and 400 °C are densely packed, significantly different from the porous feature of the film grown at 300 °C, or of the film grown at low DMZn flow rate. This observation tells that even though the growth temperature suppresses the lateral growth of ZnO nanorods, we can still enhance the lateral growth to form densely packed film at temperature above 350 °C with the help of high DMZn flow rate of 0.58 sccm while maintaining the major (0 0 0 2) oriented growth direction.

Although the grain size increases as temperature increases from 350 °C to 400 °C, the increased grain size does not bring us significant crystal alignment improvement, as the XRD (0 0 0 2) peak intensity is still at the same order as that of the other peaks such as $(1\,0\,\bar{1}\,1)$. This suggests significant amount of ZnO grains still have their *c*-axis tilted somewhat away from the substrate normal. This may be caused by the premature coalescence of nuclei at high growth temperatures. The possible premature coalescence of nuclei at high growth temperatures can be illustrated by the model shown in Fig. 3. The high temperature causes the enhanced coalescence of nuclei, the coalescence of nuclei causes the formation of tilted grains, and the subsequent grain growth causes the tilted crystallographic orientations of final grains with respect to the substrate, as seen from the right-hand side of the figure. If the nucleus can be left undisturbed initially, and let the coalescence effect take place at later stage, the coalescence may have minimal effect on the disturbance of the grain orientation, as seen from the left-hand side of the figure.

A two-step growth approach is taken to establish the well-aligned nuclei at lower temperatures (350 °C) and to grow and sinter these grains at higher temperatures (400 °C). If the preceding model is correct, the two-step growth approach may improve the (0 0 0 2) crystal alignment of the ZnO film. Thus

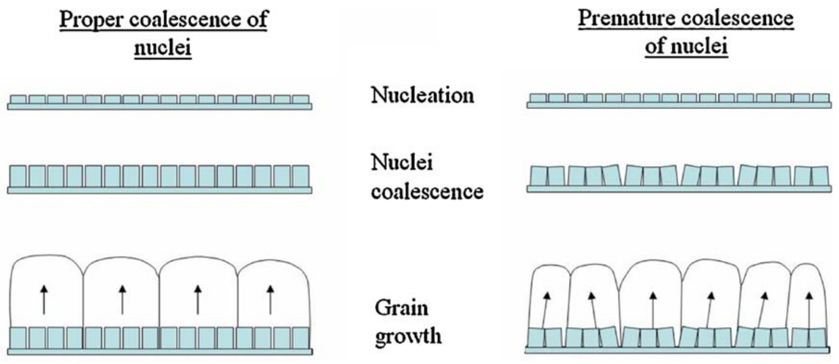

Fig. 3. Schematic of the film growth sequences. Going from nucleation, to coalescence, to grain growth, the left-hand-side figure represents ideal growth condition by proper coalescence of nuclei, and the right-hand-side figure represents tilted grain formation due to premature coalescence of nuclei grown at high temperature.

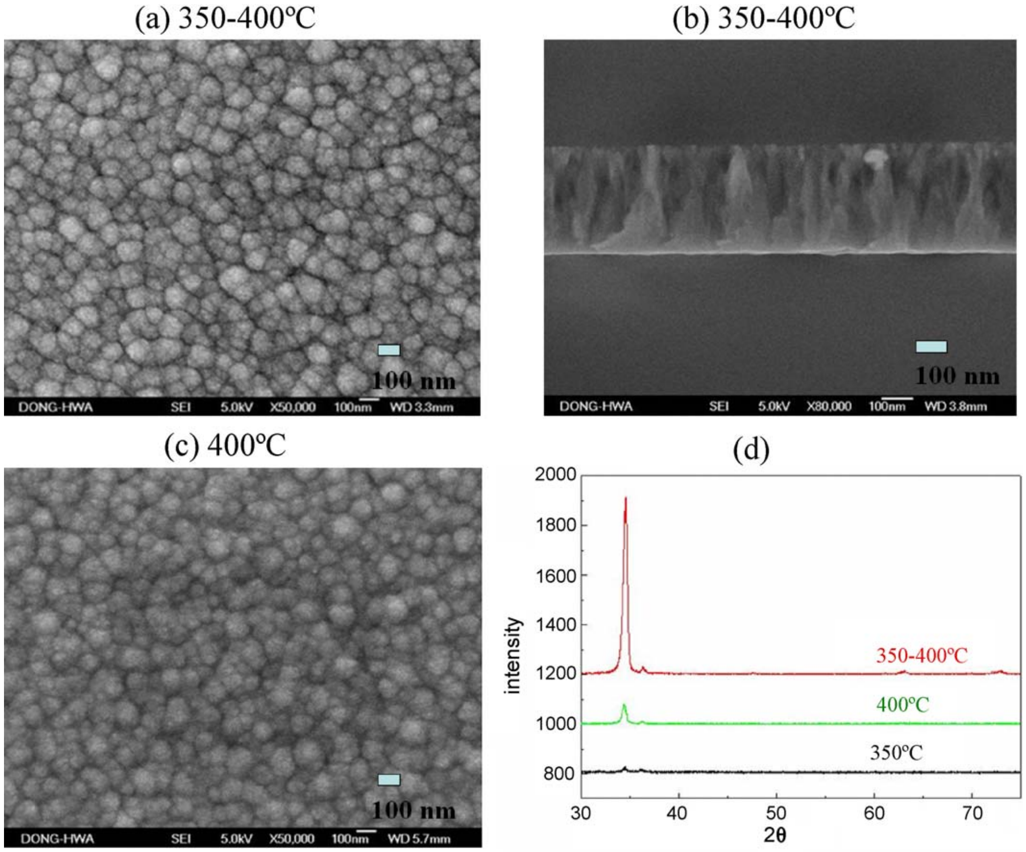

Fig. 4. The film morphology of ZnO grown by two-step method. (a) Top view of film by two-step growth of 350–400 °C, (b) side view of film by two-step growth of 350-400 °C, (c) top view of film grown by single-step growth of 400 °C (same as Fig. 1(c), shown here for easy comparison), and (d) XRD spectrum of film by two-step growth of 350–400 °C along with those for films grown at 400 °C and 350 °C for comparison.

growth is performed under the temperature control that the temperature rises linearly from 350 °C to 400 °C for the first 5 min, and maintained at 400 °C for the rest of the 20-min growth duration. The film morphology is shown in Fig. 4(a) (top view) and Fig. 4(b) (side view). It can be seen that the average grain size is much larger than grains isothermally grown at 350 °C [Fig. 1(b)], and comparable to the grains isothermally grown at 400 °C [Fig. 1(c)]. The XRD peak at (0 0 0 2) is much higher than those isothermally grown either at 350 °C or 400 °C [Fig. 4(d)], indicating a superior improvement of crystal alignment by the two-step growth process. The result agrees perfectly with the growth model discussed earlier, suggesting that the high growth temperature may alter the nuclei alignment at the initial growth stage.

## 4. Conclusion

We have successfully prepared dense and continuous ZnO film by MOCVD using increased DMZn flow rate with $CO_2$ as oxygen precursor. We found that the growth temperature suppresses the lateral growth of ZnO. We also found that higher growth temperature promotes the coalescence of grains but reduces the crystal alignment. Using a two-step growth method, employing the initial growth at lower temperature followed by the growth at higher temperature, a densely packed ZnO film with larger grains and well-aligned crystallographic orientation can be achieved simultaneously.

## Acknowledgements

The authors would like to acknowledge J.M. Wu, Y.Z. Jhang, and Y.A. Su for X-ray and EM analysis and H.T. Wang of Eastern Sharp Ltd. for MOCVD system assembly. This work was mainly supported by the funding from the National Science Council of the Taiwan under the Project No. NSC-93-2215-E-259-003. The FE-SEM operation was supported by the National Science Council of Taiwan under the Project No. NSC-96-2120-M-259-001.

## References

[1] D.C. Look, D.C. Reynolds, J.R. Sizelove, R.L. Jones, C.W. Litton, G. Cantwell, W.C. Harsch, Electrical properties of bulk ZnO, Solid State Commun. 105 (1998) 399–401.

[2] N. Saito, H. Haneda, T. Sekiguchi, N. Ohashi, I. Sakaguchi, K. Koumoto, Low-temperature fabrication of light-emitting zinc oxide micropatterns using self-assembled monolayers, Adv. Mater. 14 (2002) 418–421.

[3] S. Liang, H. Sheng, Y. Liu, Z. Hio, Y. Lu, H. Shen, ZnO Schottky ultraviolet photodetectors, J. Cryst. Growth 225 (2001) 110–113.

[4] Y. Liu, C.R. Gorla, S. Liang, N. Emanetoglu, Y. Lu, H. Shen, M. Wraback, Ultraviolet detectors based on epitaxial ZnO films grown by MOCVD, J. Electron. Mater. 29 (2000) 69–74.

[5] Y. Lin, Z. Zhang, Z. Tang, F. Yuan, J. Li, Characterisation of ZnO-based varistors prepared from nanometre precursor powders, Adv. Mater. Opt. Electron. 9 (1999) 205–209.

[6] N. Golego, S.A. Studenikin, M. Cocivera, Sensor photoresponse of thin-film oxides of zinc and titanium to oxygen gas, J. Electrochem. Soc. 147 (2000) 1592–1594.

[7] L.C. Tien, P.W. Sadik, D.P. Norton, L.F. Voss, S.J. Pearton, H.T. Wang, B.S. Kang, F. Ren, J. Jun, J. Lin, Hydrogen sensing at room temperature with Pt-coated ZnO thin films and nanorods, Appl. Phys. Lett. 87 (2005) 222106.

[8] N.W. Emanetoglu, C. Gorla, Y. Liu, S. Liang, Y. Lu, Epitaxial ZnO piezoelectric thin films for saw filters, Mater. Sci. Semicond. Process. 2 (1999) 247–252.

[9] C.G. Van de Walle, Defect analysis and engineering in ZnO, Physica B 308–310 (2001) 899–903.

[10] Ü. Özgür, Ya.I. Alivov, C. Liu, A. Teke, M.A. Reshchikov, S. Doğan, V. Avrutin, S.-J. Cho, H. Morkoç, A comprehensive review of ZnO materials and devices, J. Appl. Phys. 98 (2005) 041301.

[11] J. Wang, V. Sallet, G. Amiri, J.F. Rommeluère, A. Lusson, E. Rzepka, J.E. Lewis, P. Galtier, O. Gorochov, Growth parameters and substrate treatment for the MOCVD growth of ZnO, Phys. Stat. Sol. A 202 (2005) 1967–1972.

[12] M.H. Koch, P.Y. Timbrell, R.N. Lamb, The influence of film crystallinity on the coupling efficiency of ZnO optical modulator waveguides, Semicond. Sci. Technol. 10 (1995) 1523–1527.

[13] D.C. Look, Recent advances in ZnO materials and devices, Mater. Sci. Eng. B 80 (2001) 383–387.

[14] K. Keem, H. Kim, G.T. Kim, J.S. Lee, B. Min, K. Cho, M.Y. Sung, S. Kim, Photocurrent in ZnO nanowires grown from Au electrodes, Appl. Phys. Lett. 84 (2004) 4376–4378.

[15] H. Kind, H. Yan, M. Law, B. Messer, P. Yang, Nanowire ultraviolet photodetectors and optical switches, Adv. Mater. 14 (2002) 158–160.

[16] Y. Huang, X. Duan, Y. Cui, L.J. Laubon, K.H. Kim, C.M. Lieber, Logic gates and computation from assembled nanowire building blocks, Science 294 (2001) 1313–1317.

[17] D.M. Bagnall, Y.F. Chen, Z. Zhu, T. Yao, S. Koyama, M.Y. Shen, T. Goto, Optically pumped lasing of ZnO at room temperature, Appl. Phys. Lett. 70 (1997) 2230–2232.

[18] C. Kirchner, Th. Gruber, F. Reu, K. Thonke, A. Waag, Ch. Gieβen, M. Heuken, MOVPE growth of ZnO using various oxygen precursors, J. Crystal Growth 248 (2003) 20–24.

[19] J.B. Baxter, E.S. Aydil, Epitaxial growth of ZnO nanowires on a- and c-plane sapphire, J. Cryst. Growth 274 (2005) 407–411.

[20] A. Sekar, S.H. Kim, A. Umar, Y.B. Hahn, Catalyst-free synthesis of ZnO nanowires on Si by oxidation of Zn powders, J. Cryst. Growth 277 (2005) 471–478.

[21] K.-H. Bang, D.-K. Huang, S.-W. Lim, J.-M. Myoung, Effects of growth temperature on the properties of ZnO/GaAs prepared by metalorganic chemical vapor deposition, J. Cryst. Growth 250 (2003) 437–443.

[22] T. Hirate, S. Sasaki, W. Li, H. Miyashita, T. Kimpara, T. Satoh, Effects of laser-ablated impurity on aligned ZnO nanorods grown by chemical vapor deposition, Thin Solid Films 487 (2005) 35–39.

[23] B. Hahn, G. Heindel, E. Pschorr-Schoberer, W. Gebhardt, MOCVD layer growth of ZnO using DMZn and tertiary butanol, Semicond. Sci. Technol. 13 (1998) 788–791.

[24] D.R. Gaskell, Introduction to the Thermodynamics of Materials, 4th ed., Taylor and Francis, New York, 2003, pp. 365–375.

[25] Jhih-Han Du, Preparation of dense (0 0 2)-oriented ZnO thin film by metal-organic chemical vapor deposition, Thesis, National Dong Hwa University, Shoufeng, Hualien, Taiwan, 2007.

[26] M. Ohring, Materials Science of Thin Film, 2nd ed., Academic Press, New York, 2002, p. 383.

[27] P. Smereka, X. Li, G. Russo, D.J. Srolovitz, Simulation of faceted film growth in three dimensions: microstructure, morphology and texture, Acta Mater. 53 (2005) 1191–1204.

[28] C.V. Thompson, Structure evolution during processing of polycrystalline films, Annu. Rev. Mater. Sci. 30 (2000) 159–190.